

NJC

Accepted Manuscript



This is an *Accepted Manuscript*, which has been through the Royal Society of Chemistry peer review process and has been accepted for publication.

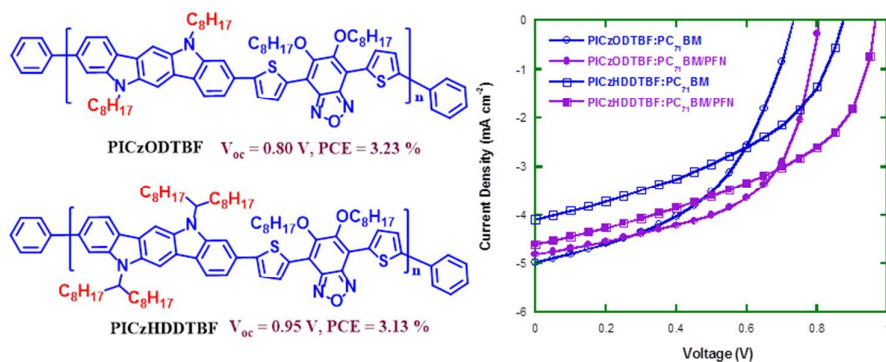
Accepted Manuscripts are published online shortly after acceptance, before technical editing, formatting and proof reading. Using this free service, authors can make their results available to the community, in citable form, before we publish the edited article. We will replace this *Accepted Manuscript* with the edited and formatted *Advance Article* as soon as it is available.

You can find more information about *Accepted Manuscripts* in the [Information for Authors](#).

Please note that technical editing may introduce minor changes to the text and/or graphics, which may alter content. The journal's standard [Terms & Conditions](#) and the [Ethical guidelines](#) still apply. In no event shall the Royal Society of Chemistry be held responsible for any errors or omissions in this *Accepted Manuscript* or any consequences arising from the use of any information it contains.

Graphical Abstract

Two indolo[3,2-b]carbazole and 5,6-bis(octyloxy)benzofurazan based narrow band-gap polymers **PICzODTBF** and **PICzHDDTBF** give the maximum power conversion efficiency of 3.32 % and 3.13 % with the open circuit voltage of 0.80 V and 0.95 V, respectively.



ARTICLE

Indolo[3,2-b]carbazole and Benzofurazan Derivative Containing Narrow Band-Gap Polymers for Photovoltaic Cells

Cite this: DOI: 10.1039/x0xx00000x

Received 00th January 2012,
Accepted 00th January 2012

DOI: 10.1039/x0xx00000x

www.rsc.org/

Bin Zhang,* Lei Yu, Li Fan, Na Wang, Liwen Hu, Wei Yang

Abstract

Two indolo[3,2-b]carbazole and 5,6-bis(octyloxy)benzofurazan based narrow band-gap polymers **PICzODTBF** and **PICzHDDTBF** with linear and branched side chains respectively were synthesized, and their optical, electrochemical and photovoltaic properties were characterized. The number-averaged molecular weight (M_n) of **PICzODTBF** and **PICzHDDTBF** are 8600 and 21400 with polydispersity index (PDI) of 1.97 and 2.43, respectively. The absorption spectra in film show that the peaks are located at 405 and 571 nm for **PICzODTBF**, and 396 and 531 nm for **PICzHDDTBF**, accompanying with the optical band gaps of 1.90 and 2.05 eV, respectively. Compared with **PICzHDDTBF**, the absorption of **PICzODTBF** is red shifted obviously resulting from its linear side chains leading to the better π - π stacking between polymer chains. Through the electrochemical characterization, the HOMO energy levels are -5.02 and -5.28 eV with LUMO energy levels of -3.09 and -3.08 eV for **PICzODTBF** and **PICzHDDTBF**, respectively. The photovoltaic devices are fabricated with the structure of ITO/PEDOT:PSS/polymer: PC₇₁BM/PFN/Al. With respect to **PICzODTBF**, the short circuit current density (J_{sc}), open circuit voltage (V_{oc}), fill factor (FF) and power conversion efficiency (PCE) are 4.81 mA cm⁻², 0.80 V, 57 % and 3.23 %, respectively. **PICzHDDTBF** has the J_{sc} , V_{oc} , FF and PCE of 4.61 mA cm⁻², 0.95 V, 48 % and 3.13 %, respectively.

Introduction

Bulk-Heterojunction polymer solar cells (BHJ-PSCs) as one kind of versatile photovoltaic technologies are attracted extensively both academically and industrially, resulting from their fantastic merits in low cost, large-scale fabrication, flexibility, light weight and so on. Recently, the high-efficiency PSCs with power conversion efficiency (PCE) exceeding 9 % are achieved which are potentially applicable in electrical power generation.^{1,2}

In BHJ-PSCs, electron-donating polymers are one of important materials which work as absorber of the incident sun light and transporting host of holes.³ Until now, there are large amount of excellent donor polymers designed and synthesized, for instance,

polyfluorenes (PFs),⁴⁻⁶ polycarbazoles (PCzs),⁷⁻⁹ polythiophenes (PThs),¹⁰ polybenzodithiophenes (PBDTs)¹¹⁻¹³ and polysilafluorenes (PSiFs)¹⁴. Some of these polymers display highly efficient photovoltaic properties through blending with fullerene derivatives as acceptor materials, such as [6,6]-phenyl-C61-butyric acid methyl ester (PC₆₁BM)¹⁵, indene-C₆₀ bisadduct (ICBA)¹⁶ and [6,6]-phenyl-C71-butyric acid methyl ester (PC₇₁BM)^{1,13}.

Indolo[3,2-b]carbazole, due to its highly thermal stability, largely aromatic planarity, lower band gap, high hole mobility and feasible functionalization, has been studied tremendously in organic light-emitting diodes (OLEDs)¹⁷ and organic field-effect transistors (OFETs)¹⁸⁻²⁰. Also, indolo[3,2-b]carbazole as good electron-donating unit has been introduced to the polymer backbones in

PSCs, where it shows that it is an advanced alternative to other donor moieties and gives the PCE over 3.0 %. ²¹⁻²⁴ On the other side, in order to construct narrow band-gap polymers, another co-monomer is indispensable. The structure of mostly used co-monomers belongs to the donor-acceptor-donor (D-A-D) type, for example, 4,7-di(thiophen-2-yl)-2,1,3-benzothiadiazole (DTBT) ⁸, 3,6-di(thiophen-2-yl)pyrrole [3,4-c]pyrrole-1,4 (2H,5H)-dione (DPP) ^{25, 26}, 3,7-Di(3-hexylthiophen-5-yl)-naphtho[1,2-c:5,6-c]bis[1,2,5]thiadiazole (DTNT) ²⁷, (E)-1,1'-bis(2-hexyldecyl)-6,6'-bis(4-octylthiophen-2-yl)-[3,3'-biindolylidene]-2,2'-dione (Isoindigole) ²⁸, 4,7-di(thiophen-2-yl)-2,1,3-benzo selenodizole (DTBSe) ²⁹. 4,7-di(thiophen-2-yl)-5,6-bis(octyloxy) benzofurazan (DFOB) as a versatile D-A-D typed co-monomer has been introduced to the polymer main chains to construct the outstanding donor polymers, ascribing to its advantageous characteristics in easy synthesis, narrow band gap and high solubility; furthermore, a high electronegative oxygen atom in benzofurazan can make the HOMO energy level deeper, which is very beneficial for the improvement of open circuit voltage (V_{oc}) in PSCs. ^{7, 30-32}

Herein, two indolo[3,2-b]carbazole derivatives containing linear or branched side chains were synthesized. Then, two alternating polymers **PICzODTBF** and **PICzHDDTBF** were prepared by polymerizing linear chains substituted 5,11-dioctylindolo[3,2-b]carbazole or branched chains substituted 5,11-di(9-heptadecanyl)indolo[3,2-b]carbazole units with DFOB moiety, and utilized as donor materials in BHJ-PSCs to evaluate their photovoltaic performance.

Experimental section

Characterization and instrumentation

¹H nuclear magnetic resonance (NMR) and ¹³C NMR measurements were carried out on a Bruker 300 MHz and 600 MHz DRX spectrometer with tetramethylsilane (TMS) as the internal reference. The number-average molecular weight (M_n) and weight-average molecular weight (M_w) were determined on a Waters gel permeation chromatography (GPC) system with linear polystyrene as standards and tetrahydrofuran (THF) as eluent. UV-vis absorption spectra were performed on a HP 8453 spectrophotometer. Cyclic voltammetry (CV) was characterized on a CHI600D electrochemical workstation with a standard three electrodes cell based on a Pt wire counter electrode and a platinum (Pt) working electrode, against

saturated calomel electrode (SCE) as reference electrode at a scan rate of 50 mV s⁻¹ within a nitrogen-saturated anhydrous solution of 0.1 mol L⁻¹ tetrabutylammonium hexafluorophosphates (Bu₄NPF₆) in acetonitrile, versus ferrocene/ferrocenium (Fc/Fc⁺) as the internal reference.

Device fabrication

All devices were fabricated on ITO-coated glass substrates. A thin layer (40 nm) of PEDOT:PSS (Clevios 4083) was spin coated onto UV-ozone treated ITO substrates at 4000 rpm for 40 s and then baked at 140 °C for 15 min in air. The solution containing the polymer (10 mg/ml) and fullerene (20 mg/ml) (polymer:fullerene = 1:2, wt/wt) in *o*-dichlorobenzene (ODCB) were spin-coated inside a glove-box with nitrogen at 1200 rpm for 40 s to form the active layers (~80 nm). For the device structure of ITO/PEDOT:PSS/active layer/poly[(9,9-dioctyl-2,7-fluorene)-alt-(9,9-bis(3'-(N,N-dimethyl amino)propyl)-2,7-fluorene)] (**PFN**)/Al, the **PFN** layer (5 nm) was prepared by spin casting a mixed solution (0.2 mg/ml) with the methanol to acetic acid volume ratio of 100:1 before the cathode evaporation. Aluminum cathode (80 nm) was then thermally evaporated under vacuum (~10⁻⁶ torr) through a shadow mask defining an active device area of 0.16 cm². The current-voltage (J-V) curves were measured by using a Keithley 2400 multimeter under AM 1.5 G solar illumination at 87 mW cm⁻² and a Thermal-Oriel 150W solar simulator. Incident photon-to-current conversion efficiency (IPCE) values were obtained with a monochromator and calibrated with a silicon photodiode. Hole mobility data of neat polymers were measured by space charge limited current (SCLC) method with the device configuration of ITO/PEDOT:PSS(40 nm)/active layer(150 nm for **PICzODTBF** and 66 nm for **PICzHDDTBF**)/MoO₃(10 nm)/Al(90 nm). Preliminarily, PEDOT:PSS was spin casted on the ITO coated glass substrate, then, active layers were prepared from ODCB solution with the 1 % concentration by spin coating. Finally, MoO₃ and Al layers were deposited by thermal evaporation under high vacuum, respectively.

Synthesis of monomers and polymers

The synthetic routes of monomers and polymers are shown in Scheme 1. 3,9- dibromoindolo[3,2-b]carbazole **1**, ²² 3,9-Dibromo-5,11-di(9-heptadecanyl)indolo[3,2-b]carbazole **4**, ²² 3,9-Bis(4,4(5,5(-tetramethyl-1(3,2(-dioxaborolan-2(-yl)-5,11-di(9-heptadecanyl) indolo[3,2-b]carbazole **5** ²² and 4,7-Bis(5-bromothiophen-2-yl)-5,6-bis(octyloxy)benzofurazan **6** ⁷ were

prepared according to the published procedures. All the other monomers and polymers were obtained by the following synthetic methodologies.

3,9-dibromo-5,11-dioctylindolo[3,2-b]carbazole 2. 3,9-dibromoindolo[3,2-b]carbazole (3.0 g, 7.24 mmol) and tetrabutylammonium bromide (233 mg, 0.724 mmol) were suspended in dimethyl sulphoxide (DMSO, 120 ml) under the nitrogen protection, and KOH aqueous solution (50 wt/wt %, 5 ml) were added dropwise. Heated the mixture to 80 °C and reacted for 1 hour. Then, 1-bromooctane (4.3 g, 21.72 mmol) was added in one portion. When 1-bromooctane was added completely, the reaction was continued in 80 °C for additional 3 hours. Cooled it to room temperature, and poured the mixture to water; then filtered off, washed by ethanol, and dried it at 60 °C in vacuum. The yellow solid (4.5 g) was obtained, yielding 97 %. ¹H-NMR (300 MHz, CDCl₃, δ), 8.03 (d, 2H,), 7.95(s, 2H), 7.54 (s, 2H), 7.33 (d, 2H), 4.34 (t, 4H), 1.93 (t, 4H), 1.44~1.26 (br, 20H), 0.85 (t, 6H). ¹³C-NMR (75 MHz, CDCl₃, δ), 142.47, 136.28, 122.47, 121.70, 121.31, 121.17, 119.52, 111.49, 99.00, 43.46, 31.82, 29.40, 29.21, 28.73, 27.33, 22.61, 14.07.

3,9-Bis(4,4(5,5(-tetramethyl-1(3,2(-dioxaborolan-2(-yl)-5,11-dioctylindolo[3,2-b] carbazole 2 (5.13 g, 8.03 mmol), bis(pinacolato)diboron (6.1 g, 24.1 mmol), Pd(dppf)₂Cl₂ (293 mg, 0.4 mmol) and KOAc (8.6 g, 80.3 mmol) were dissolved in dioxane (250 ml), and purified by nitrogen for three times. Then, heated the mixture to 80 °C and reacted for 48 hours. Stopped the reaction and filtered off in hot to remove the insoluble inorganics. The solvent dioxane was removed in vacuum and crude product was obtained. The crude product was recrystallized in a mixed solution of THF and methanol, and acquired golden powder 5.7 g, yielding 97 %. ¹H-NMR (300MHz, CDCl₃, δ), 8.24 (d, 2H,), 8.04 (s, 2H), 7.89 (s, 2H), 7.70 (d, 2H), 4.45 (t, 4H), 1.96 (t, 4H), 1.43~1.28 (br, 20H), 0.87 (t, 6H). ¹³C-NMR (75MHz, CDCl₃, δ), 141.27, 136.54, 125.33, 124.18, 123.43, 123.18, 119.53, 114.67, 99.13, 83.74, 43.24, 31.86, 29.44, 29.26, 28.91, 27.32, 24.96, 22.64, 14.09.

Poly(3,9-(5,11-dioctylindolo[3,2-b]carbazole)-alt-4,7di(thiophen-2-yl)-5,6-bis(octyloxy)benzofu razan) PICzODTBF. 3,9-Bis(4,4(5,5(-tetramethyl-1(3,2(-dioxaborolan-2(-yl)-5,11-dioctylindolo[3,2-b] carbazole 3 (366 mg, 0.5 mmol), 4,7-bis(5-bromothiophen-2-yl)-5,6-bis(octyloxy) benzofurazan 6 (349 mg, 0.5

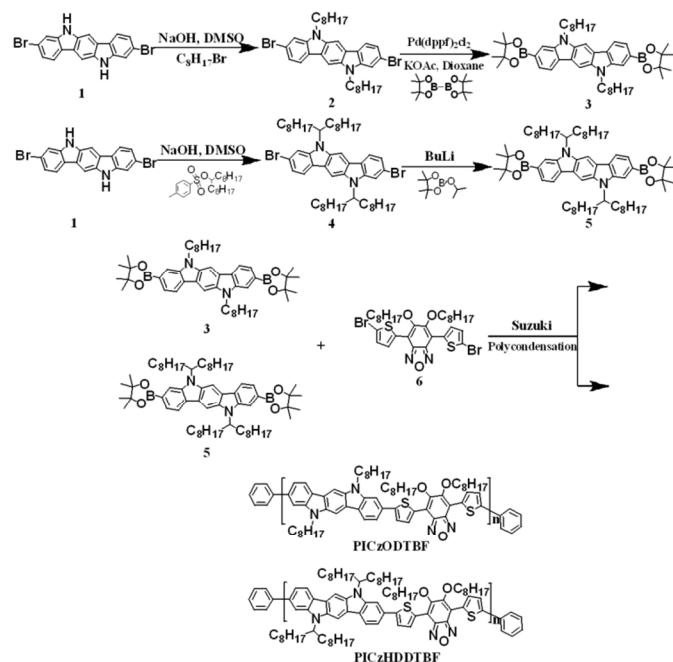
mmol), Pd(PPh₃)₄ (11.6 mg, 0.01 mmol) were dissolved in 40 ml toluene under the argon protection. Then, tetraethylammonium hydroxide (2 ml, 20 wt/wt% in water) was added in one portion at room temperature. Heated the reaction to 85 °C and reacted at this temperature for 48 hours. Phenylboronic acid (609 mg, 5 mmol) was added and reacted for 12 hours at 85°C; then, bromobenzene (1.570 g, 10 mmol) was added in one portion and reacted for additional 12 hours. Cooled it to room temperature and precipitated in methanol. The crude polymer was purified by Soxlet extraction in methanol, acetone, hexane and chloroform respectively; the final chloroform solution was precipitated in methanol. Filtered off and dried at 60 °C in the vacuum oven for 12 hours, and got 0.171g red solid, yielding 34 %. ¹H-NMR (600 MHz, *d*-ODCB, δ), 8.15~6.84 (br, 8H), 6.57~6.31 (m, 4H), 4.10~3.67 (br, 4H), 1.76~1.48 (m, 4H), 1.24~1.16 (br, 48H), 0.90~0.78 (m, 12H). GPC (THF): *M_n* = 8600, *M_w* = 16900, PDI = 1.97.

Poly(3,9-(5,11-di(9-heptadecanyl)indolo[3,2-b]carbazole)-alt-4,7-di(thiophen-2-yl)-5,6-bis(octyloxy)benzofu razan) PICzHDDTBF. 3,9-Bis(4,4(5,5(-tetramethyl-1(3,2(-dioxaborolan-2(-yl)-5,11-di(9-heptadecanyl) indolo[3,2-b]carbazole 5 (296 mg, 0.3 mmol), 4,7-bis(5-bromothiophen-2-yl)-5,6-bis(octyloxy)benzofurazan 6 (210 mg, 0.3 mmol), Pd(PPh₃)₄ (6.90 mg, 0.006 mmol) were dissolved in 15 ml toluene under the argon protection. Then, tetraethylammonium hydroxide (2 ml, 20 wt/wt% in water) was added in one portion at room temperature. Heated the reaction to 85 °C and reacted at this temperature for 48 hours. Phenylboronic acid (0.609 g, 5 mmol) was added and reacted for 12 hours at 85°C; then, bromobenzene (1.570 g, 10 mmol) was added in one portion and reacted for additional 12 hours. Cooled it to room temperature and precipitated in methanol. The crude polymer was purified by Soxlet extraction in methanol, acetone, hexane and chloroform respectively; the final chloroform solution was precipitated in methanol. Filtered off and dried at 60 °C in the vacuum oven for 12 hours, and got 332 mg red solid, yielding 53 %. ¹H-NMR (600 MHz, CDCl₃, δ), 8.58 (s, 2H), 8.26~7.61 (m, 10H), 4.80~4.75 (m, 2H), 4.35~4.29 (br, 4H), 1.64~1.50 (m, 4H), 1.43~1.36 (m, 8H), 1.28~1.19 (br, 68H), 0.94~0.82 (m, 18H). GPC (THF): *M_n* = 21400, *M_w* = 52000, PDI = 2.43.

Results and discussion

Synthesis

The detailed synthetic routes are displayed in Scheme 1. The monomer 3,9-Bis(4(4,5(5-(tetramethyl-1(3(2-(dioxaborolan-2-yl)-5,11-dioctylindolo[3,2-b] carbazole 3 was synthesized by Suzuki coupling reaction in the presence of bis(pinacolato)diboron, resulting from the very low solubility of 3,9-dibromo-5,11- dioctylindolo[3,2-b] carbazole 2 at low temperature if prepared by the BuLi. **PICzODTBf** and **PICzHDDTBf** were synthesized by Suzuki polycondensation in toluene, and purified by Soxhlet extraction in methanol, acetone, hexane and chloroform for 12 h each, and then precipitated in methanol, dried at 60 °C under vacuum for 12 h. The solubility of polymers are good in common organic solvents (such as tetrahydrofuran, chloroform, chlorobenzene, dichlorobenzene). The gel permeation chromatography (GPC) characterization shows that the number-averaged molecular weight (M_n) and polydispersity index (PDI) are 8600, 1.97 and 21400, 2.43 for **PICzODTBf** and **PICzHDDTBf** respectively. (See Table 1) Compared with **PICzHDDTBf**, **PICzODTBf** has lower molecular weight which is possibly because the existence of only two linear octyl side chains and large planarity in indolo[3,2-b]carbazole unit limits the polymer's solubility when polymerization and ultimately inhibits the increment of molecular weight. However, **PICzHDDTBf** with two branched heptadecanyl side chains in indolo[3,2-b]carbazole unit can enhance its solubility dramatically and improve molecular weight feasibly.



Scheme 1 Synthetic routes of monomers and polymers.

Table 1 Molecular weight and thermal stability

polymer	M_n	M_w	PDI	T_d (°C)
PICzODTBf	8600	16900	1.97	324
PICzHDDTBf	21400	52000	2.43	333

Thermal stability

The thermal stability of polymers is a very indispensable parameter for estimating performance of BHJ-PSCs. The temperatures at 5 % weight loss in thermal gravimetric analysis (See Fig. 1) of **PICzODTBf** and **PICzHDDTBf** are 324 and 333 °C respectively, (See Table 1) which indicate that these two polymers have good thermal stability.

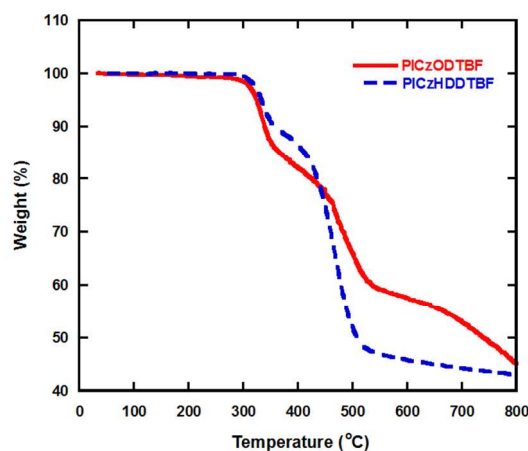


Fig. 1 Thermal gravimetric analysis curves of **PICzODTBf** and **PICzHDDTBf**.

Absorption and electrochemical analysis

The UV-vis absorption spectra of polymers in chloroform and in film are shown in Fig. 2a. Each of these two polymers has two distinct absorption peaks both in solution and in film; ones of the peaks are located at around 400 nm due to the localized π - π^* transition, and other peaks at longer wavelength which are attributed to the internal charge transfer interaction between the donor and acceptor units are ranged from about 530 to 570 nm. (See Table 2) Compared to the **PICzHDDTBf**, **PICzODTBf** exists obvious larger red shift in film than in chloroform, which is shifted from 398 and 535 nm in chloroform to the 405 and 571 nm in film, respectively. This larger red shift in **PICzODTBf** is possibly ascribed to its better intermolecular π - π stacking resulting from its more linear side chains than the branched heptadecanyl side chains in **PICzHDDTBf**. The onsets of absorption spectra of

PICzODTBF and **PICzHDDTBF** in film are 654 and 606 nm, which correspond to the optical band gaps of 1.90 and 2.05 eV, respectively.

The cyclic voltammogram (CV) characterization in Fig. 2b presents the reversibly oxidative and reductive curves, in which the onsets of oxidation and reduction potentials for **PICzODTBF** and **PICzHDDTBF** are located at 0.42, -1.51 and 0.68, -1.52 V versus SCE, respectively. The redox potential of Fc/Fc⁺ internal reference is 0.2 V vs. SCE. The highest occupied molecular orbit (HOMO) and the lowest unoccupied molecular orbit (LUMO) energy levels of **PICzODTBF** and **PICzHDDTBF**, determined by calculating from the empirical formula of $E_{\text{HOMO}} = -e(E_{\text{ox}} + 4.8 - E_{1/2, (\text{Fc/Fc}^+)})$ and $E_{\text{LUMO}} = -e(E_{\text{re}} + 4.8 - E_{1/2, (\text{Fc/Fc}^+)})$, are -5.02, -3.09 and -5.28, -3.08 eV, respectively. In contrast, the higher HOMO energy level of **PICzODTBF** than **PICzHDDTBF** is possibly ascribing to the compact configuration in **PICzODTBF** substituted by the straight side chains in indolocarbazole segments.^{33,34} The energy band gaps of **PICzODTBF** and **PICzHDDTBF** calculated from CV data are 1.93 and 2.20 eV respectively, which are approximate to the optical band gaps (See Table 2).

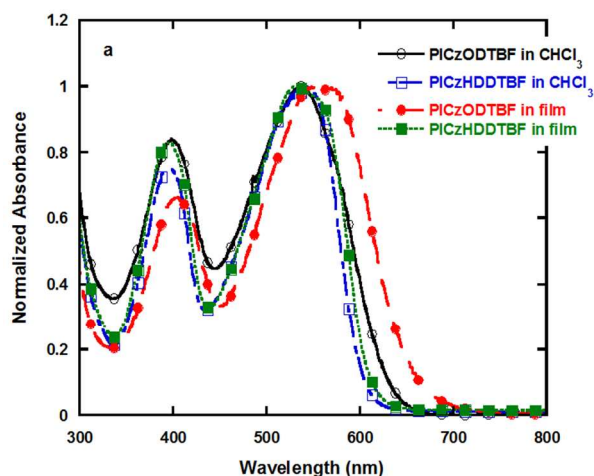


Table 2 UV-vis absorption and electrochemical properties

polymer	λ_{max} , in chloroform (nm)	λ_{max} , in film (nm)	λ_{onset} (nm)	$E_{\text{g, optical}}$ (eV)	E_{ox} (V)	E_{re} (V)	E_{HOMO} (eV)	E_{LUMO} (eV)	$E_{\text{g, CV}}$ (eV)
PICzODTBF	398, 535	405, 571	654	1.90	0.42	-1.51	-5.02	-3.09	1.93
PICzHDDTBF	395, 530	396, 531	606	2.05	0.68	-1.52	-5.28	-3.08	2.20

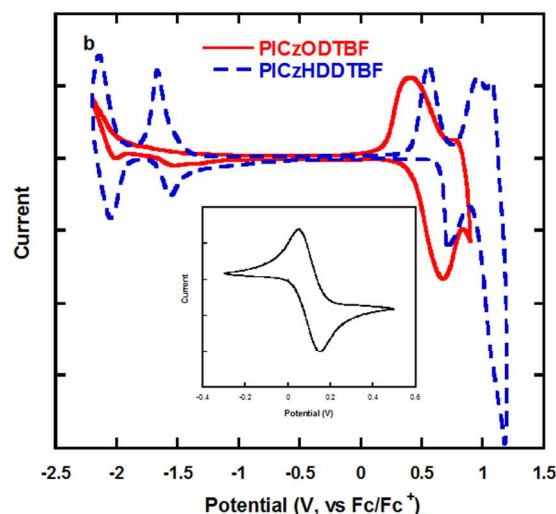


Fig. 2 UV-vis absorption spectra of **PICzODTBF** and **PICzHDDTBF** in chloroform and in film (a) and cyclic voltammogram curves of **PICzODTBF** and **PICzHDDTBF** in film (b) (inset: graph of the ferrocene oxidative curve).

Hole mobility

The hole mobility of neat polymers, were measured by the space charge limited current (SCLC) method with the device configuration of ITO/PEDOT:PSS/active layer/MoO₃/Al. Fig. 3 shows the J–V curves of neat polymer films from SCLC devices. The hole mobilities of **PICzODTBF** and **PICzHDDTBF** are 2.4×10^{-4} and $2.7 \times 10^{-5} \text{ cm}^2 \text{ V}^{-1} \text{ s}^{-1}$, respectively. In contrast with **PICzHDDTBF**, **PICzODTBF** has higher hole mobility which is possibly because of its better intermolecular π – π stacking resulting from its more linear side chains than branched side chains in **PICzHDDTBF**, and ultimately, this strong stacking effect can strengthen the hole transporting ability between polymer chains.

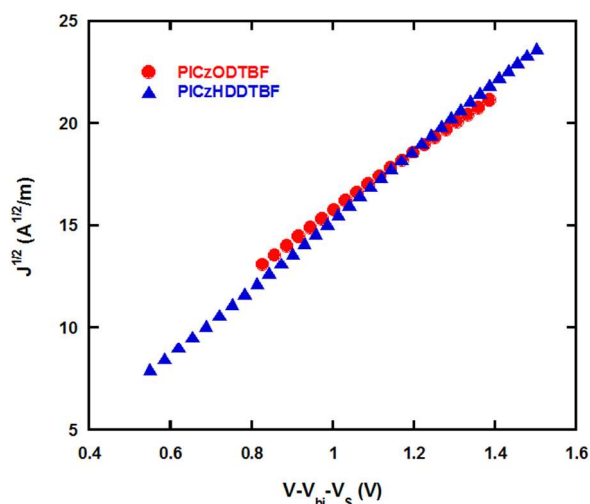


Fig. 3 J - V characteristics of **PICzODTBF** and **PICzHDDTBF** films from SCLC devices.

Photovoltaic properties

PSCs were fabricated with the device architecture of ITO/PEDOT:PSS/polymer:PC₇₁BM/(PFN)/Al. Here, PC₇₁BM was selected as acceptor material resulting from its better light absorption in visible region, and PFN was utilized as a cathode interfacial layer attributing to its versatile functions in protecting active layer when cathode evaporating and possibly existing the built-in electric fields between active layer and cathode.^{35,36} The current density–voltage (J - V) curves are shown in Fig. 4a. It displays that **PICzODTBF** based PSCs have larger short circuit current density (J_{sc}) which is possibly attributing to its better light absorption than **PICzHDDTBF**. On the other side, **PICzHDDTBF** based PSCs have higher open circuit voltage (V_{oc}) than **PICzODTBF**. This is possibly because that **PICzHDDTBF** has deeper HOMO energy level than **PICzODTBF**, where the value of V_{oc} is proportional to the energy level difference between HOMO energy level of donor and LUMO energy level of acceptor.³⁷ Furthermore, by inserting **PFN** as the cathode interfacial layer, the V_{oc} and fill factor (FF) are enhanced distinctly, and therefore, resulted in the enhancement of PCEs. The incident photon-to-current conversion efficiency (IPCE) curves of PSCs are shown in Fig. 4b. The IPCE which use **PFN** as the cathode interfacial layer is similar to the ones without **PFN** layer. In comparison to **PICzHDDTBF** based PSCs, the **PICzODTBF** based ones have broadened and enhanced IPCE in the visible region ascribing to its intensified and broadened light absorption.

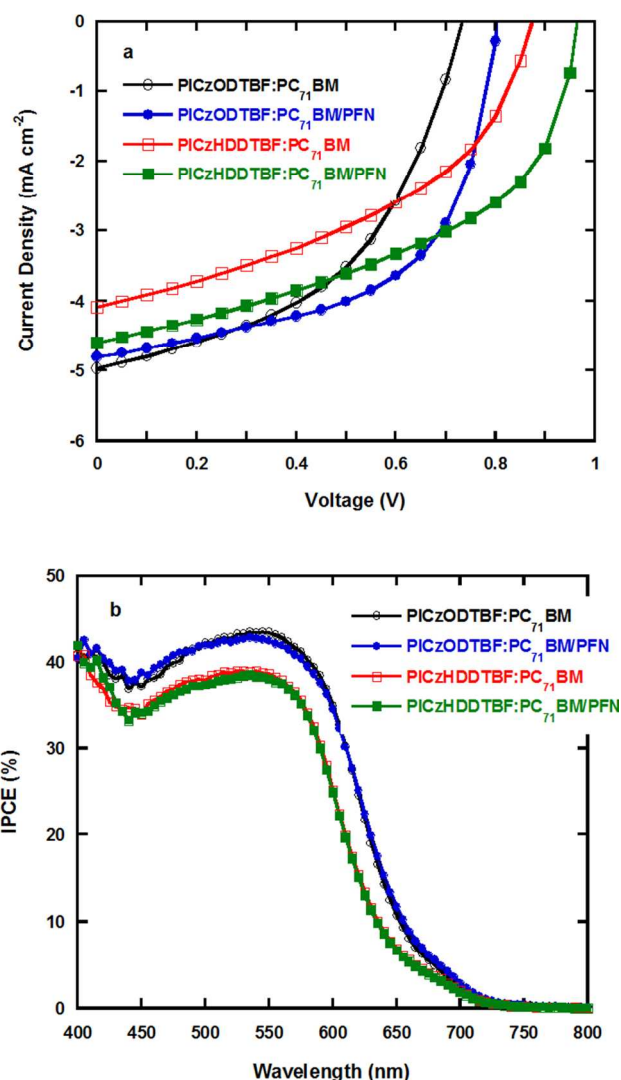


Fig. 4 Current density–voltage (J - V) characteristics of polymers:PC₇₁BM under AM 1.5 G, 87 mW cm⁻² (a); incident photon-to-current conversion efficiency (IPCE) curves of polymers:PC₇₁BM blend films (b).

The photovoltaic performance in detail under AM 1.5 G, 87 mW cm⁻² are summarized in Table 3. It shows that **PICzHDDTBF** based solar cells have higher V_{oc} values, in which the highest V_{oc} can reach to 0.95 V; nevertheless, the **PICzODTBF** based PSCs have higher J_{sc} of 4.89 mA cm⁻² and higher FF of 57 %. Ultimately, both of **PICzODTBF** and **PICzHDDTBF** based photovoltaic devices exist similar PCEs of 3.23 % and 3.13 %, respectively.

Table 3 Photovoltaic performances under AM 1.5 G, 87 mW cm⁻²

active layer (1:2, wt/wt)	cathode	J _{sc} (mA cm ⁻²)	V _{oc} (V)	FF (%)	PCE (%)
PICzODTBF :PC₇₁BM	Al	4.89	0.75	48	2.60
	PFN/Al	4.81	0.80	57	3.23
PICzHDDTBF :PC₇₁BM	Al	4.09	0.85	45	2.30
	PFN/Al	4.61	0.95	48	3.13

AFM morphology

AFM images of the blend films are shown in Figure 5. In the topography of Figure 5a-b, the root-mean-square (RMS) roughness of **PICzODTBF** and **PICzHDDTBF** based blend films are 1.659 and 4.348 nm respectively, which means that **PICzHDDTBF**:PC₇₁BM film is rougher than **PICzODTBF** based one. Moreover, the phase images (Figure 5c-d) display that **PICzODTBF**:PC₇₁BM film gives the better nano-scale phase separation,³⁸ while **PICzHDDTBF** based one shows worse phase separation and forms small islands that would affect negatively holes and electrons transportation and ultimately affect the photovoltaic properties. Also, according to the photovoltaic performance in Table 3, it depicts that **PICzODTBF** based PSCs exhibit higher FF due to the better nano-scale phase separation in **PICzODTBF**:PC₇₁BM blend films.

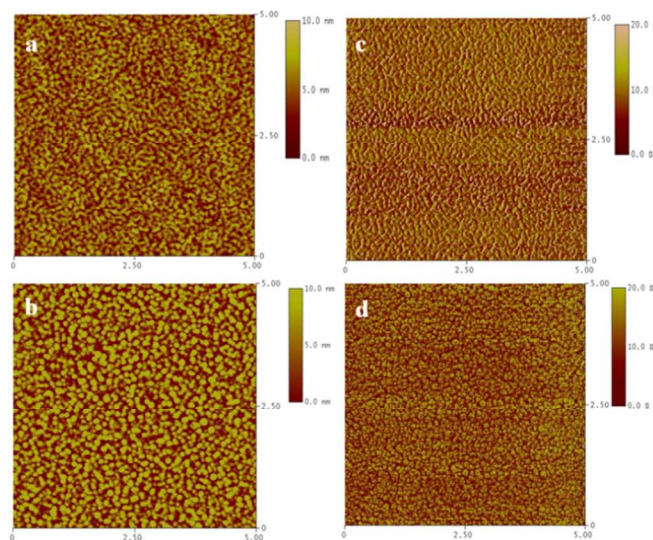


Fig. 5 AFM images of blend films (1:2 weight ratio), topography of **PICzODTBF**:PC₇₁BM (a) and **PICzHDDTBF**:PC₇₁BM (b); phase images of **PICzODTBF**:PC₇₁BM (c) and **PICzHDDTBF**:PC₇₁BM (d)

Conclusions

In summary, two indolo[3,2-b]carbazole derived narrow band-gap polymers **PICzODTBF** and **PICzHDDTBF** with different side chains were designed and prepared by Suzuki polycondensation. The **PICzODTBF** with linear chains shows higher J_{sc} values than **PICzHDDTBF** ascribing to its better light absorption which is resulted from better intermolecular π - π stacking between polymer chains. However, branched side chains anchored polymer **PICzHDDTBF** exists higher V_{oc} values due to its deeper HOMO energy level. Therefore, it is a feasible method by side chain engineering to tune energy levels and band gaps of conjugated polymers. Moreover, these results approve that indolo[3,2-b]carbazole is possibly potential candidate to design and synthesize narrow band-gap polymeric donors for highly efficient PSCs.

Acknowledgements

This work was financially supported by the National Nature Science Foundation of China (Nos. 51273069, 51303056), the Research Fund for the Doctoral Program of Higher Education of China (No. 20130172110005) and the Fundamental Research Funds for the Central Universities (No. 2014ZB0017).

Notes and references

Institute of Polymer Optoelectronic Materials and Devices, State Key Laboratory of Luminescent Materials and Devices, South China University of Technology, Guangzhou 510640, China. E-mail: mbszhang@scut.edu.cn

- 1 Z. C. He, C. M. Zhong, S. J. Su, M. Xu, H. B. Wu and Y. Cao, *Nat. Photonics*, 2012, **6**, 591.
- 2 J. B. You, L. T. Dou, K. Yoshimura, T. Kato, K. Ohya, T. Moriarty, K. Emery, C. C. Chen, J. Gao, G. Li and Y. Yang, *Nat. Commun.*, 2013, **4**, 1446.
- 3 Y. F. Li, *Acc. Chem. Res.*, 2012, **45**, 723.
- 4 O. Inganäs, F. L. Zhang, K. Tvingstedt, L. M. Andersson, S. Hellstrom and M. R. Andersson *Adv. Mater.*, 2010, **22**, E100.
- 5 M. Wang, C. H. Li, A. F. Lv, Z. H. Wang and Z. S. Bo, *Macromolecules*, 2012, **45**, 3017.
- 6 C. Du, C. H. Li, W. W. Li, X. Chen, Z. S. Bo, C. Veit, Z. F. Ma, U.

- Wuerfel, H. F. Zhu, W. P. Hu and F. L. Zhang, *Macromolecules*, 2011, **44**, 7617.
- 7 B. Zhang, X. W. Hu, M. Q. Wang, H. P. Xiao, X. Gong, W. Yang and Y. Cao, *New J. Chem.*, 2012, **36**, 2042.
- 8 N. Blouin, A. Michaud and M. Leclerc, *Adv. Mater.*, 2007, **19**, 2295.
- 9 R. P. Qin, W. W. Li, C. H. Li, C. Du, C. Veit, H. F. Schleiermacher, M. Andersson, Z. S. Bo, Z. P. Liu, O. Inganäs, U. Wuerfel and F. L. Zhang, *J. Am. Chem. Soc.*, 2009, **131**, 14612.
- 10 L. J. Huo and J. H. Hou, *Polym. Chem.*, 2011, **2**, 2453.
- 11 Y. Y. Liang, Y. Wu, D. Q. Feng, S. T. Tsai, H. J. Son, G. Li and L. P. Yu, *J. Am. Chem. Soc.*, 2009, **131**, 56.
- 12 J. H. Hou, H. Y. Chen, S. Q. Zhang, R. I. Chen, Y. Yang, Y. Wu and G. Li, *J. Am. Chem. Soc.*, 2009, **131**, 15586.
- 13 H. Y. Chen, J. H. Hou, S. Q. Zhang, Y. Y. Liang, G. W. Yang, Y. Yang, L. P. Yu, Y. Wu and G. Li, *Nat. Photonics*, 2009, **3**, 649.
- 14 E. G. Wang, L. Wang, L. F. Lan, C. Luo, W. L. Zhuang, J. B. Peng and Y. Cao, *Appl. Phys. Lett.*, 2008, **92**, 033307.
- 15 Y. Y. Liang and L. P. Yu, *Acc. Chem. Res.*, 2010, **43**, 1227.
- 16 Y. J. He, H. Y. Chen, J. H. Hou and Y. F. Li, *J. Am. Chem. Soc.*, 2010, **132**, 1377.
- 17 S. Lengvinaite, J. V. Grazulevicius, S. Grigalevicius, R. Gu, W. Dehaen, V. Jankauskas, B. Zhang and Z. Xie, *Dyes Pigm.*, 2010, **85**, 183.
- 18 Y. N. Li, Y. L. Wu and B. S. Ong, *Macromolecules*, 2006, **39**, 6521.
- 19 Y. L. Wu, Y. N. Li, S. Gardner and B. S. Ong, *J. Am. Chem. Soc.*, 2005, **127**, 614.
- 20 P. T. Boudreault, S. Wakim, N. Blouin, M. Simard, C. Tessier, Y. Tao and M. Leclerc, *J. Am. Chem. Soc.*, 2007, **129**, 9125.
- 21 Y. J. Xia, X. H. Su, Z. C. He, X. Ren, H. B. Wu, Y. Cao and D. W. Fan, *Macromol. Rapid Commun.*, 2010, **31**, 1287.
- 22 E. J. Zhou, S. P. Yamakawa, Y. Zhang, K. Tajima, C. Yang and K. Hashimoto, *J. Mater. Chem.*, 2009, **19**, 7730.
- 23 J. P. Lu, F. S. Liang, N. Drolet, J. F. Ding, Y. Tao and R. Movileanu, *Chem. Commun.*, 2008, 5315.
- 24 J. H. Tsai, C. C. Chueh, M. H. Lai, C. F. Wang, W. C. Chen, B. T. Ko and C. Ting, *Macromolecules*, 2009, **42**, 1897.
- 25 W. W. Li, W. S. C. Roelofs, M. M. Wienk and R. A. J. Janssen, *J. Am. Chem. Soc.*, 2012, **134**, 33, 13787.
- 26 J. C. Bijleveld, A. P. Zoombelt, S. G. J. Mathijssen, M. M. Wienk, M. Turbiez, D. M. de Leeuw and R. A. J. Janssen, *J. Am. Chem. Soc.*, 2009, **131**, 16616.
- 27 M. Wang, X. W. Hu, P. Liu, W. Li, X. Gong, F. Huang and Y. Cao, *J. Am. Chem. Soc.*, 2011, **133**, 9638.
- 28 E. G. Wang, Z. F. Ma, Z. Zhang, O. Vandewal, P. Henriksson, O. Inganäs, F. L. Zhang and M. R. Andersson, *J. Am. Chem. Soc.*, 2011, **133**, 14244.
- 29 W. Zhao, W. Z. Cai, R. X. Xu, W. Yang, X. Gong, H. B. Wu and Y. Cao, *Polymer*, 2010, **51**, 3196.
- 30 P. Ding, C. M. Zhong, Y. P. Zou, C. Y. Pan, H. B. Wu and Y. Cao, *J. Phys. Chem. C*, 2011, **115**, 16211.
- 31 J. M. Jiang, P. A. Yang, H. C. Chen and K. H. Wei, *Chem. Commun.*, 2011, **47**, 8877.
- 32 J. M. Jiang, P. A. Yang, T. H. Hsieh and K. H. Wei, *Macromolecules*, 2011, **44**, 9155.
- 33 E. G. Wang, L. T. Hou, Z. Q. Wang, Z. F. Ma, S. Hellström, W. L. Zhuang, F. L. Zhang, O. Inganäs and M. R. Andersson, *Macromolecules*, 2011, **44**, 2067.
- 34 E. G. Wang, J. Bergqvist, K. Vandewal, Z. F. Ma, L. T. Hou, A. Lundin, S. Himmelberger, A. Salleo, C. Müller, O. Inganäs, F. L. Zhang and M. R. Andersson, *Adv. Energy Mater.*, 2013, **3**, 806.
- 35 C. He, C. M. Zhong, H. B. Wu, R. Q. Yang, W. Yang, F. Huang, G. C. Bazan and Y. Cao, *J. Mater. Chem.*, 2010, **20**, 2617.
- 36 Z. C. He, C. M. Zhong, X. Huang, W. Y. Wong, H. B. Wu, L. W. Chen, S. J. Su and Y. Cao, *Adv. Mater.*, 2011, **23**, 4636.
- 37 M. C. Scharber, D. Mühlbacher, M. Koppe, P. Denk, C. Waldorf, A. J. Heeger and C. J. Brabec, *Adv. Mater.*, 2006, **18**, 789.
- 38 J. Zhao, Y. J. He, Y. F. Li, *Adv. Mater.*, 2010, **22**, 4355.